Journal of Biomolecular Structure and Dynamics

ISSN: (Print) (Online) Journal homepage: https://www.tandfonline.com/loi/tbsd20

Naringenin-4'-glucuronide as a new drug candidate against the COVID-19 Omicron variant: a study based on molecular docking, molecular dynamics, MM/PBSA and MM/GBSA

Alexandre de Fátima Cobre, Moisés Maia Neto, Eduardo Borges de Melo, Mariana Millan Fachi, Luana Mota Ferreira, Fernanda Stumpf Tonin & Roberto Pontarolo

To cite this article: Alexandre de Fátima Cobre, Moisés Maia Neto, Eduardo Borges de Melo, Mariana Millan Fachi, Luana Mota Ferreira, Fernanda Stumpf Tonin & Roberto Pontarolo (2023): Naringenin-4'-glucuronide as a new drug candidate against the COVID-19 Omicron variant: a study based on molecular docking, molecular dynamics, MM/PBSA and MM/GBSA, Journal of Biomolecular Structure and Dynamics, DOI: 10.1080/07391102.2023.2229446

To link to this article: https://doi.org/10.1080/07391102.2023.2229446

JOURNAL OF BIOMOLECULAR STRUCTURE AND DYNAMICS
https://doi.org/10.1080/07391102.2023.2229446

Naringenin-4′-glucuronide as a new drug candidate against the COVID-19 Omicron variant: a study based on molecular docking, molecular dynamics, MM/PBSA and MM/GBSA

Alexandre de Fátima Cobre[a], Moisés Maia Neto[b], Eduardo Borges de Melo[c], Mariana Millan Fachi[a], Luana Mota Ferreira[d], Fernanda Stumpf Tonin[e] and Roberto Pontarolo[d]

[a]Pharmaceutical Sciences Postgraduate Programme, Universidade Federal do Paraná, Curitiba, Brazil; [b]Department of Pharmacy, Fametro University Centre (UNIFAMETRO), Fortaleza-Ceará, Brazil; [c]Department of Pharmacy, Universidade Estadual do Oeste do Paraná (UNIOESTE), Cascavel-PR, Brazil; [d]Department of Pharmacy, Universidade Federal do Paraná, Curitiba, Brazil; [e]H&TRC - Health & Technology Research Centre, ESTeSL, Escola Superior de Tecnologia da Saúde, Instituto Politécnico de Lisboa, Lisbon, Portugal

Communicated by Ramaswamy H. Sarma

ABSTRACT

This study aimed to identify natural bioactive compounds (NBCs) as potential inhibitors of the spike (S1) receptor binding domain (RBD) of the COVID-19 Omicron variant using computer simulations (*in silico)*. NBCs with previously proven biological *in vitro* activity were obtained from the ZINC database and analyzed through virtual screening, molecular docking, molecular dynamics (MD), molecular mechanics/Poisson–Boltzmann surface area (MM/PBSA), and molecular mechanics/generalized Born surface area (MM/GBSA). Remdesivir was used as a reference drug in docking and MD calculations. A total of 170,906 compounds were analyzed. Molecular docking screening revealed the top four NBCs with a high affinity with the spike (affinity energy $<$-7 kcal/mol) to be ZINC000045789238, ZINC000004098448, ZINC000008662732, and ZINC000003995616. In the MD analysis, the four ligands formed a complex with the highest dynamic equilibrium S1 (mean RMSD $<$0.3 nm), lowest fluctuation of the complex amino acid residues (RMSF $<$1.3), and solvent accessibility stability. However, the ZINC000045789238-spike complex (naringenin-4′-O glucuronide) was the only one that simultaneously had minus signal (-) MM/PBSA and MM/GBSA binding free energy values (-3.74 kcal/mol and $-$15.65 kcal/mol, respectively), indicating favorable binding. This ligand (naringenin-4′-O glucuronide) was also the one that produced the highest number of hydrogen bonds in the entire dynamic period (average = 4601 bonds per nanosecond). Six mutant amino acid residues formed these hydrogen bonds from the RBD region of S1 in the Omicron variant: Asn417, Ser494, Ser496, Arg403, Arg408, and His505. Naringenin-4′-O-glucuronide showed promising results as a potential drug candidate against COVID-19. *In vitro* and preclinical studies are needed to confirm these findings.

Abbreviations: ACE-2: angiotensin converting enzyme 2; CADD: computer-aided drug discovery; CHARMM: chemistry at Harvard macromolecular mechanics; COVID-19: coronavirus disease 2019; GROMACS: groningen machine for chemical simulations; HIV: human immunodeficiency virus; LINCS: linear constraint solver; MD: molecular dynamics; MM/GBSA: molecular mechanics/generalised Born surface area; MM/PBSA: molecular mechanics/Poisson–Boltzmann surface area; NBCs: natural bioactive compounds; NVE: microcanonical; NPT: isothermal-isobaric; NVT: canonical; PDB: protein data bank; PDBQT: protein data bank partial charge and atom type format; QSAR: quantitative structure-activity relationship; RBD: receptor binding domain; RCSB: research collaboratory for structural bioinformatics; Rg: radius of gyration; RMSD: root mean square deviation; RMSF: root mean square fluctuation; SASA: solvent accessible surface area; S1: subunit 1 spike glycoprotein; SARS-CoV-2: Severe acute respiratory syndrome coronavirus 2; VMD: visual molecular dynamics; WHO: world health organisation

ARTICLE HISTORY
Received 12 January 2023
Accepted 19 June 2023

KEYWORDS
Naringenin-4′-glucuronide; SARS-CoV-2; treatment; spike protein; in silico

1. Introduction

Two years into the global COVID-19 pandemic, with over 591 million infections and more than 6.5 million confirmed deaths by August 2022 (WHO, 2022), the focus of attention has shifted to the emergence and spread of new variants of SARS-CoV-2 that have now been associated with substantial detrimental effects on the transmission and severity of the virus (Liu et al., 2022).

The Omicron variant (B.1.1.529), initially detected in Southern Africa in November 2021, became a dominant strain of concern, given its high transmissibility (Liu et al., 2022; Mannar et al., 2022; WHO, 2021). Due to the significant accumulation of mutations in the receptor binding domain

CONTACT Roberto Pontarolo pontarolo@ufpr.br Department of Pharmacy, Universidade Federal do Paraná, Campus III, Av. Pref. Lothário Meissner, 632, Jardim Botânico, Curitiba, PR 80210-170, Brazil

Supplemental data for this article can be accessed online at https://doi.org/10.1080/07391102.2023.2229446.

(RBD) of the spike protein of the virus (Cao et al., 2022), this variant has greater resistance to neutralizing antibodies, whether from patients recovered from COVID-19 or vaccinated individuals (Cao et al., 2022; Liu et al., 2022).

In this context, the repositioning of drugs or even the discovery of potential new drugs capable of curing or preventing diseases is an attractive, immediate, and realistic approach to tackle the ongoing COVID-19 pandemic (Sultana et al., 2020; Venkatesan, 2021). The discovery of pharmacological activity through high-throughput screening of potential compounds available in databases is an emerging strategy that has already led to the approval of new indications for marketed drugs (*e.g.*, lopinavir/ritonavir for HIV) and the development of therapeutic options repositioned against Ebola, hepatitis C and Zika virus (Y. Kumar et al., 2020; Villas-Boas et al., 2020).

Few studies targeting computer-aided drug discovery (CADD) for COVID-19 are available in the literature, most of which were developed using the molecular targets of the wild virus or other mutations of SARS-CoV-2. This approach may impact the therapeutic success of the drug candidates, as in the case of hydroxychloroquine, which showed promising results in preclinical studies for disease repositioning, but had no additional benefits in clinical trials (poor efficacy and safety profile).

This study aimed to search for a potential inhibitor of the spike protein (S1) RBD of the Omicron variant of SARS-CoV-2 through computer simulations (*in silico)* of molecular docking, molecular dynamics (MD), molecular mechanics/Poisson–Boltzmann surface area (MM/PBSA) and molecular mechanics/generalized Born surface area (MM/GBSA), using a bank of more than 170,000 natural bioactive compounds (NBCs).

2. Material and methods

The three-dimensional structure of the spike glycoprotein (S1) of the Omicron variant of SARS-CoV-2 was obtained from the Research Collaboratory for Structural Bioinformatics protein data bank (RCSB PDB), which is a public domain database (Berman et al., 2007). The spike (S1) target was selected because of the SARS-CoV-2-RBD fragment that interacts with human ACE-2, which is responsible for the recognition and penetration of the virus in lung cells (Yan et al., 2020). Several S1 glycoproteins obtained from the RCSB PDB database were pre-evaluated, considering: (i) the result of the validation percentage ranking; (ii) the availability of information on the RBD with human ACE-2; and (iii) the presence of a complete amino acid sequence. PDB ID 7T9L was the only structure selected for evaluation, given its completeness with the abovementioned three criteria (Yan et al., 2020).

2.1. Protein target preparation

The 3D structure of the spike (S1) glycoprotein with the Omicron mutation (PDB ID 7T9L) (Mannar et al., 2022) in the PDB format was prepared in the Autodock tools software, where (i) all crystallization water molecules were removed by X-ray to avoid steric hindrance at the time of docking with the ligands; (ii) the polar hydrogens were added; and (iii) the Kolman charges were included (Ravi & Kannabiran, 2016). Finally, we investigated the protonation state of the titratable amino acids of the spike protein (S1) RBD at pH 7.4 using Open Babel software (O'Boyle et al., 2011). After preparation, the molecule file was converted to the PDBQT format. Discovery Studio Visualizer Software was used to visualize the prepared protein structure (Yan et al., 2020).

2.2. Identification of amino acid residues in the RBD region of the spike protein (S1)

After the preparation of the molecular target (PDB ID 7T9L), the original scientific article of the molecular target structure (PDB ID 7T9L) was carefully read (Mannar et al., 2022), aiming to identify which amino acid residues of the spike protein structure (S1) of the Omicron variant interact with human ACE-2, *i.e.*, the amino acid residues of the RBD. In the next step, the mutant amino acid residues of the RBD of the variant were identified by comparing the amino acid sequences of the spike protein (S1) RBD wild type (PDB ID 6M17) (Yan et al., 2020) with the amino acid sequence of the spike protein (S1) RBD of the molecular target in the study (PDB ID 7T9L). A total of fifteen amino acid residues were identified as the S1 RBD spike residues of the Omicron mutation, namely, Asp339, Asp339, Pro373, Phe375, Asn417, Lys440, Ser446, Asn477, Lys478, Ala484, Arg493, Ser496, Ar498, TyR501 and His505 (Supplementary file, Table S1).

2.3. Collection and preparation of ligands

A total of 170,906 commercially available natural bioactive molecules were obtained from the ZINC15 database (Sterling & Irwin, 2015). The ZINC database was chosen because it is the only database with filters to select only commercially available compounds and is a very used database in drug discovery (Irwin & Shoichet, 2005). This filter allows these compounds to be purchased and tested *in vitro* or *in vivo*. These compounds have shown biological activity against other diseases *in vitro* studies. These compounds were obtained in 3D structure in a mol2 format file, which is recognized in most *in silico* study software.

All ligands were prepared in PyRx virtual screening tolls using two steps (Dallakyan & Olson, 2015). The first step was the minimization of the energy of each ligand using the following parameters: (i) force field: UFF; (ii) optimization algorithm: conjugate gradients; (iii) the total number of steps: 200; (iv) number of steps for update: 1; stop if energy difference is less than 0.1, to obtain its most stable conformation, which could be used to interact with the target protein. We also assigned Gasteiger partial charges to all ligands using AutoDoCk Raccoon software (Gasteiger & Marsili, 1980). After that, we also investigate the protonation state of all ligands at pH 7.4 using Open Babel software (O'Boyle et al., 2011).

The second step was the conversion of the format of the ligand files from 'mol2' to the 'PDBQT' format, using AutodockVina software, which is coupled with the PyRx virtual screening tools software.

2.4. Virtual screening and molecular docking

Before performing the virtual screening (PyRx virtual screening tools), the coordinates of the center X, Y, Z and the size (angstrom) of X, Y, Z of the grid-box and the exhaustiveness of the Autodock tools and AutodockVina were adjusted. The most promising bioactive compounds were those that had both lower protein and ligand binding energy values (Kirchmair et al., 2008). The ligands with the most favorable results during the virtual screening analyses were docked using Autodock Tools 4.2.0 and AutodockVina software (Allouche, 2011; Ravi & Kannabiran, 2016). The reason for using two different software in the docking analysis (Autodock tools 4.2.0 and AutodockVina) was to evaluate the performance and accuracy of the docking results (Cuzzolin et al., 2015; Vieira & Sousa, 2019). The ligand-protein complexes with a higher binding affinity greater than −7 kcal/mol were considered for further analyses. The affinity energy cutoff value was based on published literature (Alnajjar et al., 2020; Hosseini & Amanlou, 2020; Rafi et al., 2022). The drug remdesivir was used as a reference to compare the results of molecular docking and virtual screening between our ligands with the RBD of SARS-CoV-2.

The virtual screening and molecular docking were performed using the following parameters: (i) exhaustiveness of 16; (ii) coordinates of the center of the grid-box were optimized at $x = 228.052$, $y = 172.488$, and $z = 253.630$; and (iii) the grid-box size was optimized at $x = 50$ Å, $y = 70$ Å, $z = 50$ Å. It is essential to highlight that the size of our grid-box is similar to the grid-box of the recent docking study published by Liu (2023) (Liu, 2023), who also used the same crystallographic structure of the Spike protein used in our study (PDB ID: 7T9L). In docking modeling, the search for the conformations (poses) of the ligands with the highest binding stability with the spike protein (RBD) was performed using a scoring function called the sum of parameterized energies and a random search function called a genetic algorithm. In this analysis, the protein and ligand binding energy results were compared with the root mean square deviation (RMSD) values to validate the results obtained in the virtual screening analyses (Ravi & Kannabiran, 2016).

2.5. Molecular dynamics (MD)

The ligand-protein complexes showing promising results in the docking and drug-likeness analyses were subjected to MD simulations with the S1 protein. In the ZINC database, all ligands have their partial charges calculated (Gasteiger partial charges). As the ligands used in this study were obtained from the ZINC database, in the molecular dynamics simulations, the partial charges of the ligands were not calculated (Tingle et al., 2023). The interaction energies between the amino acid residues of the spike (S1) protein were necessary to achieve an equilibrium stage. The drug remdesivir was also used as a reference to compare molecular dynamics simulation results between our ligands with SARS-CoV-2 RBD.

A 20 Å cubic water model was used for the MD tests. The spike protein (S1) was inserted in this model, together with chloride (Cl^-) and sodium (Na^+) ions, at physiological concentrations of 0.15 mol/L to neutralize the charges. The optimization of the geometries consisted of a series of sequential steps, namely, minimization, heating, and pressurization, and this process took place before the equilibrium simulation in the microcanonical (NVE) set. The simulations were performed applying the following parameters: (i) HOH angle and OH bond distance of TIP3P water molecules (SHAKE algorithm), vibration restriction in covalent bonds and periodic boundary conditions; (ii) time steps equal to 2 fs; (iii) 9.0 A electrostatic interaction cutoff for all stages of MD simulation (Field et al., 2000).

All geometries were submitted to two stages of dynamic equilibrium for a period of 10 ns, the first with a constant temperature (NVT) of 310 K and the second with continuous pressure (NPT) at 1.0 atm (between 100-200 ns, depending on its stabilization). MD simulations were performed using the Charm-36 force compound (July 2021 version) with cubic interpolation implementation. The readjustment of hydrogen bonds was performed by the linear constraint solver (LINCS) method, using the 2.0 software and the CHARMM force field (Chemistry at Harvard Macromolecular Mechanics) (Cheatham et al., 1995; Hess et al., 1997; Phillips et al., 2005). Finally, MD simulations were conducted for 100 ns, where the following MD metrics were evaluated: RMSD, mean square fluctuation (RMSF), hydrogen bonding, radius of gyration (Rg), solvent accessible surface area (SASA), temperature, pressure, density and potential (Islam et al., 2020; Y. Kumar et al., 2020; Oany et al., 2020; Rakib et al., 2020). It is essential to point out that in the MD simulations (including the calculation of the free energies of MM/PBSA and MM/GBSA), 2000 frames were used.

MD results (such as RMSD and RMSF values) were plotted in Graph Prism software. VMD (visual molecular dynamics) software was used to visualize the results of the MD simulations (Humphrey et al., 1996).

2.6. Molecular mechanics/generalized Born surface area (MM/GBSA) binding free energy calculation

The MM/GBSA calculations (equations 1, 2, and 3) were performed by gmx-mmpbsa in GROMACS (Valdés-Tresanco et al., 2021).

$$\Delta G_{bind} = \Delta H - T\Delta S = \Delta E_{MM} - T\Delta S + \Delta G_{sol} \quad \text{(Eq. 1)}$$

$$\Delta G_{MM} = \Delta E_{vdw} = \Delta E_{internal} + \Delta E_{ele} \quad \text{(Eq. 2)}$$

$$\Delta G_{sol} = \Delta G_{SA} + \Delta G_{GB} \quad \text{(Eq. 3)}$$

Where: $T\Delta S$, $\Delta E_{MM,}$ and ΔG_{sol} are, respectively, the conformational entropy, gas phase MM energy, and solvation-free energy (the sum of the nonpolar contribution ΔG_{SA} and the polar contribution ΔG_{GB}). ΔE_{MM} contains dihedral energies, electrostatic ΔE_{ele} and $\Delta E_{internal}$ of the bond, Van Der Waals energy ΔE_{vdw} and angle. The entropy calculation can be omitted if no structural changes are caused by bonds in the MD simulation process.

2.7. Molecular mechanics/Poisson–Boltzmann surface area (MM/PBSA) binding free energy calculation

The MM/PBSA method was used to determine the binding free energy of the MD simulation trajectories. The main parameters controlling the MM/PBSA calculation include (i) surface tension to estimate the nonpolar solvation energy using the evaluable surface area of the solvent, 0.054; (ii) internal dielectric constant, 1, and external dielectric constant, 80. Equations 4 and 5 below were used to calculate the MM/PBSA:

$$\Delta G_{bind} = \Delta G_{complex\,(minimised)} - \left[\Delta G_{ligand\ \ (minimised)} + \Delta G_{receptor\,(minimised)}\right] \quad \text{(Eq. 4)}$$

$$\Delta G_{bind} = \Delta G_{MM} + \Delta G_{PB} + \Delta G_{SA} - T\Delta S \quad \text{(Eq. 5)}$$

where: $T\Delta S$ = entropy contribution; ΔG_{MM} = sum between electrostatic and der Vander Waals interactions; ΔG_{SA} = nonpolar solvation energy; ΔG_{PB} = polar solvation energy.

Additionally, we performed new calculations of post-molecular dynamics simulations, where the following metrics were calculated: the distance (Å) from the center of mass per frame of the Spike protein-ligand complex and the binding free energies (MM/PBSA and MM/GBSA) per frame. It is essential to highlight that the post-MD calculations were performed using a time of 20 nanoseconds, and this time was chosen according to scientific studies previously published in the literature (Elsbaey et al., 2021; Pang et al., 2021).

2.8. Prediction of pharmacokinetic properties (ADME) and drug-likeness

For the ligands that showed a better binding affinity with the spike protein in molecular dynamics simulations, predictions of drug-likeness characteristics and pharmacokinetic parameters [absorption, distribution, metabolism, excretion (ADME)] were performed using the online platform called ADMETLAB2, which uses a machine learning algorithm (artificial neural networks or deep learning) with >85% accuracy (Xiong et al., 2021). Predictions of drug-likeness were performed using Pfizer pharmaceuticals and golden triangle rules. By Pfizer's Methodology, compounds with a high LogP (>3) and low TPSA (<75) have low oral absorption and increased toxicity. By the golden triangle method, compounds with low molecular weight (200 g/mol $\leq$ MW $\leq$50 g/mol) and low logD (-2 $\leq$ logD $\leq$ 5) have a favorable ADMET profile, that is, they are drug-like (Xiong et al., 2021). The consensus between both rules was used to define whether a molecule was drug-like, being drug-like compounds those that fulfilled both rules.

2.9. Toxicity prediction

Ligands with the highest binding affinity for the spike protein also predicted their acute and chronic toxicities using the PROTOX II online platform (Banerjee et al., 2018). Four different groups of toxicity will be predicted: (i) Organ Toxicity: Hepatotoxicity; (ii) Toxicity endpoints: Carcinogenicity, Mutagenicity, and Cytotoxicity; (iii) Tox21 Nuclear receptor signalling pathways: Aryl hydrocarbon Receptor (AhR); Androgen Receptor (AR); Androgen Receptor Ligand Binding Domain (AR-LBD); Aromatase, Estrogen Receptor Alpha (ER), Estrogen Receptor Ligand Binding Domain (ER-LBD), Peroxisome Proliferator Activated Receptor Gamma (PPAR-Gamma); (iv) Tox21 Stress response pathways: Nuclear factor (erythroid-derived 2)-like 2/antioxidant responsive element (nrf2/ARE); Heat shock factor response element (HSE), Mitochondrial Membrane Potential (MMP), Phosphoprotein (Tumor Suppressor) p53, and ATPase family AAA domain containing protein 5 (ATAD5).

3. Results

3.1. Virtual screening and molecular docking

From a total of 17,000 ligands, we selected the top four ligands with the best binding affinity with the spike protein (S1) in the virtual screening (PyRx - virtual screening) and molecular docking processes (AutoDock tools and AutoDockVina): ID ZINC000045789238 (naringenin-4′-O-glucuronide) (Figure 1E), ID ZINC000003995616 (ergoloid) (Figure 1F), ID ZINC000004098448 (ohioensin A) (Figure 1G) and ID ZINC000008662732 (prunetrin) (Figure 1H) (Table 1). The result of Molecular docking between rendersevir and the spike protein is shown in Figure 2.

All four ligands interacted with the amino acid residues of the RBD region of the Omicron variant, with the ligand naringenin-4′-O-glucuronide (Figure 1E) being the one with the highest number of hydrogen bonds ($n = 5$) with the amino acid residues of the RBD region of the Omicron mutation (Ser494, Ser496, Thr500, Thr5051, and Thr505). Prunetrin (Figure 1H) was the ligand with the second highest number of hydrogen bonds (Arg408, Asp417, Ser496, and His505), as depicted in Figure 1.

Nine conformations were obtained in the docking analyses for each of the four selected ligands. Only the conformation with the highest binding stability with the molecular target was selected (*i.e.*, conformation with an RMSD value lower than 2) (Table 1).

In this study, the coefficients of variation of the binding energies of the spike protein with the top four promising compounds obtained in the different software (PyRx, AutoDock tools, and AutoDockVina) were <2%, showing the reliability and precision of the molecular docking results (Table 1).

Table 2 compares spike protein-ligand complex interactions from virtual screening and molecular docking analyses. We can observe that in both analyses (virtual screening and molecular docking), ZINC000045789238 formed hydrogen bonds involving the amino acids Ser496, Thr500, and His505 of the RBD of the spike protein (S1). The ligand ZINC000003995616 interacted with the amino acids Ser496 (carbon-hydrogen bond) and Tyr501 (pi-pi-shaped) of the RBD region of the spike protein (S1). The ligand ZINC000004098448 established pi-alkyl and pi-pi T-shaped interactions with the amino acids Lys478, Phe486, and Val483, respectively. Finally, the ligand ZINC000003995616 interacted with the amino acids Arg408, Asn417, and Tyr453 from RBD, producing hydrogen bonds, hydrogen bonds, and carbon-hydrogen bonds, respectively. We can observe a

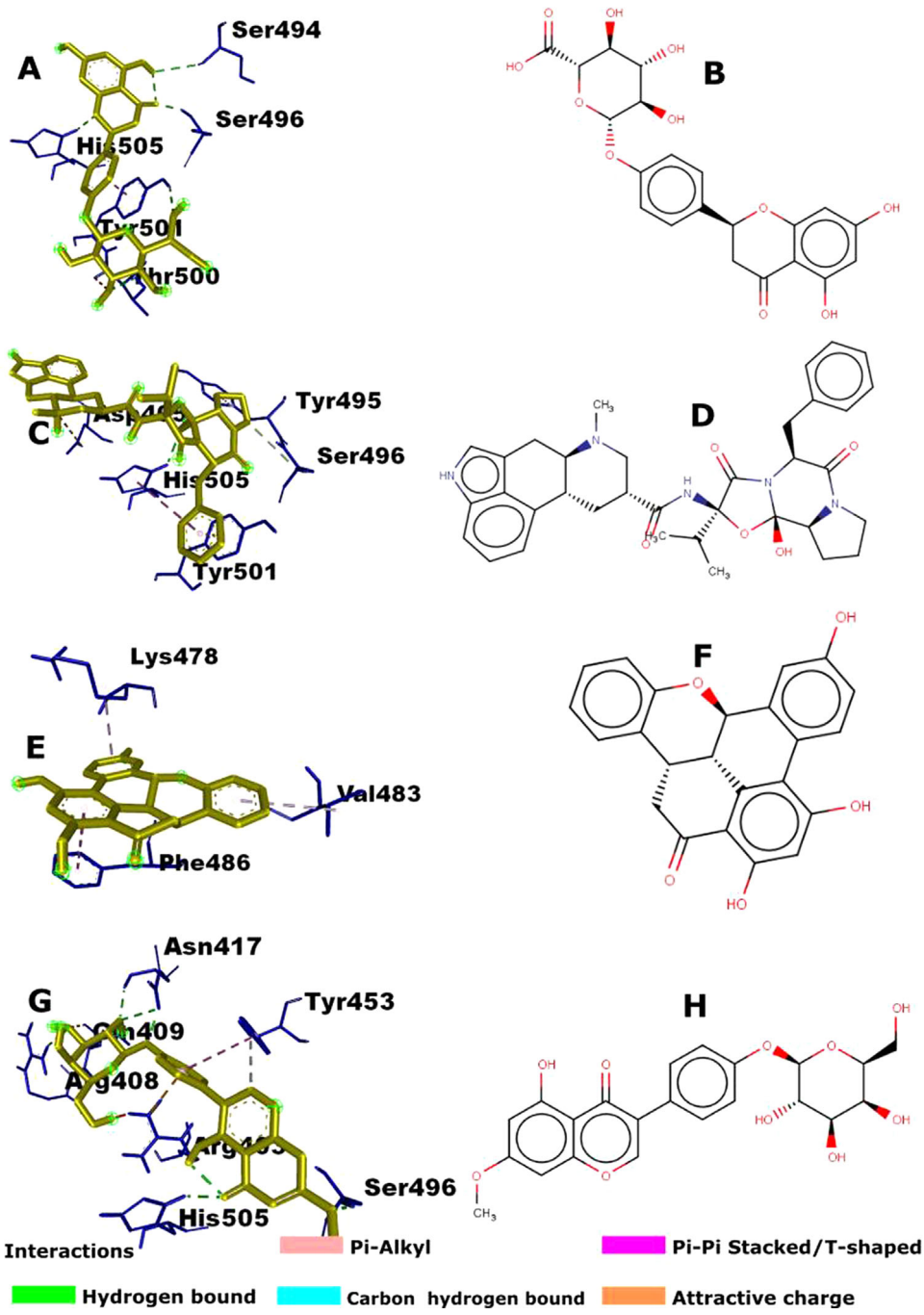

Figure 1. Molecular docking modeling of the top four ligands. The docking of the ligands naringenin-4′-O-Glucuronide (ZINC000045789238), ergoloid (ZINC000003995616), ohioensin A (ZINC000004098448), and prunetrin (ZINC000008662732) are shown in figures A, C, E and G, respectively. Yellow and blue-colored structures represent the ligands and the spike protein (S1), respectively. Spike protein-ligand complex interactions are shown in dashed lines, where the green, blue, purple, and pink lines represent hydrogen bonds, attractive charges, pi-pi stacked/PiPi-T-shaped, and pi-alkyl, respectively. Figures B, D, F, and H represent the chemical structures of naringenin-4′-O-Glucuronide (ZINC000045789238), ergoloid (ZINC000003995616), ohioensin A (ZINC000004098448) and prunetrin (ZINC000008662732), respectively, are shown.

similarity in the interactions of the protein-ligand complex in the virtual screening and molecular docking analyses.

Table 3 compares the interactions of the molecular docking analyses using the exhaustiveness of 16 and 100. In the table, we can observe that in both exhaustiveness, some RBD amino acids (Ser496, Thr500, Tyr501, and His505) were involved in the link between the ZINC000045789238 ligand and the spike protein *via* a hydrogen bond, carbon-hydrogen bond, pi-pi T-shaped and pi-pi-stacked. The ZINC000003995616-spike complex were the following amino acids by Hydrogen bond, attractive charge, pi-alkyl, carbon-hydrogen bond, pi-pi stacked and pi-pi T-shaped involving the following RBD amino acids: Asp405, Tyr495, Ser496, Tyr501. The ZINC000004098448-spike complex was formed *via* pi-alkyl and pi-pi T shaped bonds involving the following RBD amino acids: Lys478, Val483, and Phe486 by such bonds. And finally, the ZINC000008662732-Spike complex was formed through attractive charge, Hydrogen bond, carbon-hydrogen, pi-sigma, alkyl, and pi-alkylenvel bonds, including the following amino acid residues: Arg403, Arg408, Gln409,

Table 1. Virtual screening and molecular docking of the main natural compounds and the spike protein (S1) of SARS-CoV-2.

Ligand	PyRx-virtual screening		AutoDock Tools		AutodockVina	
ZINC ID	(kcal/mol)	RMSD	(kcal/mol)	RMSD	(kcal/mol)	RMSD
ZINC000004098448	−8.3	0.0	−8.9	1.1	−8.6	1.1
ZINC000045789238	−8.5	0.0	−8.8	1.3	−8.9	1.4
ZINC000008662732	−8.2	0.0	−8.7	1.1	−8.5	1.2
ZINC000003995616	−8.7	0.0	−8.3	1.4	−8.4	1.2

Note: All binding energy and RMSD values were based on the most stable conformation of the ligand after docking. Binding affinities are expressed as the lowest binding energies obtained in kcal/mol (<-7 kcal/mol). Virtual screening was obtained by PyRx-AutodockVina; Molecular docking was obtained by AutoDock1.5.6 and AutodockVina. Naringenin-4′-O-Glucuronide (ZINC000045789238), ergoloid (ZINC000003995616), ohioensin A (ZINC000004098448) and prunetrin (ZINC000008662732).

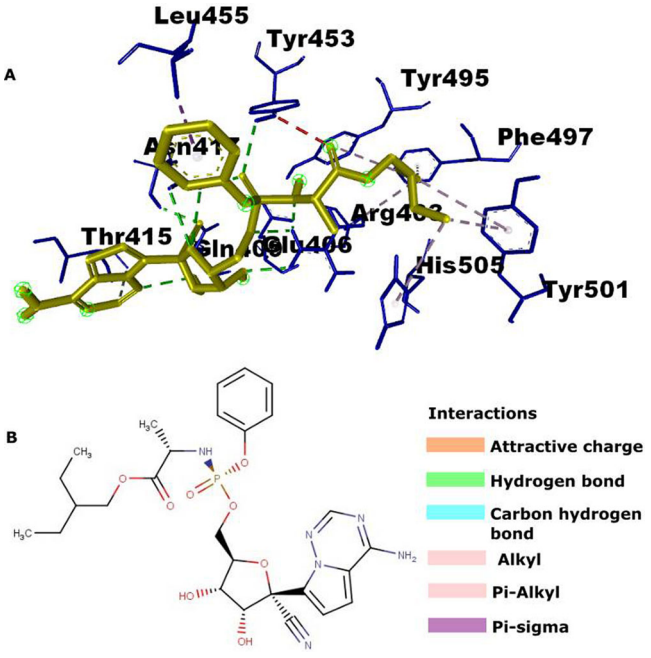

Figure 2. Molecular docking modeling of remdesivir (reference drug). spike protein-ligand complex interactions are shown in dashed lines. Yellow and blue-colored structures represent remdesivir and the spike protein (S1), respectively. The colors orange, green, light pink, and purple represent the bonds of the type tractive charges, hydrogen bonds, carbon-hydrogen bond, alkyl, pi-alkyl, and pi-sigma, respectively.

Asn417, Tyr453, Ser496, His505. 2D structures of interactions between the four ligands with the spike protein are shown in the supplementary material (page S2).

3.2. Molecular dynamics (MD)

MD simulations for each spike glycoprotein (S1) complex of the Omicron variant with the four ligands (ZINC000045789238, ZINC000004098448, ZINC000008662732, and ZINC000013374469) and remdesivir (reference drug) were conducted for 100 ns. The results of the MD simulations for four ligands and for remdesivir are shown in Figures 3 and 4, respectively. All four protein-ligand complexes had RMSD values lower than 0.3, showing that there was binding stability between the amino acid residues of the spike protein (S1) of the RBD region during the entire dynamics period: ZINC000045789238-spike(S1) complex RMSD 0.124 − 0.250 nm and mean RMSD = 0.242 nm; ZINC000004098448-spike(S1) complex RMSD 0.122 − 0.251 nm and mean RMSD = 0.232 nm; ZINC000008662732-spike(S1) complex RMSD 0.116 − 0.285 nm and mean RMSD = 0.246; ZINC000003995616-spike(S1) RMSD (0.125 − 0.308 nm) and mean RMSD = 0.264 nm (Figure 3). The average RMSD value of the remdesivir-RBD spike protein complex was 0.2417 nm (Figure 4), also showing binding stability of the complex formed (RMSD < 0.3), and these results are similar to those found with the four ligands in our study (Figure 3A).

The dynamic behavior of the amino acid residues of the spike glycoprotein (S1) was also studied by calculating the RMSF values. Although all amino acid residues of the spike glycoprotein (S1) showed fluctuations within the tolerated limit (RMSF < 1.3 nm), the amino acid residues of the Omicron mutation produced the largest fluctuations, especially Phe375, Lys440, Lys478, and Phe375 (Figure 3). For the ZINC000045789238-spike complex, five amino acid residues were identified in this analysis, three belonging to the Omicron mutation (Phe375, Lys440, Lys478) and two non-mutant residues (His519 and Ser530). In the ZINC000003995616-spike(S1) complex, the amino acid residues that underwent the most fluctuation were Arg408, Lys478, Ser530, His519, and Ser530. For the ZINC000004098448-spike (S1) complex, seven amino acids showed more alterations, four of them involved in the Omicron mutation (Leu371, Proina373, Lys440, Lys478) and three non-mutant residues (Arg408, His519 and Ser530). For the ZINC000008662732-spike (S1) complex, three mutant amino acids (Lys478, Ala484 and Phe375) and five non-mutant amino acids (Pro330, Arg346, Arg408, Ala486 and Ser530) were identified. Figure 4B shows the RMSF results for remdesivir, and we can see that five RBD amino acid residues (Arg346, Arg357, Arg408, His519, and Ser519) that showed higher RMSF values (greater fluctuation) were the same amino acid residues that also showed greater fluctuations in the four ligands identified in this study.

The ZINC000045789238-spike complex had the highest number of hydrogen bond interactions (total = 46007 hydrogen bonds), with an average of 4601 bonds per nanosecond of dynamics, and the following amino acid residues establishing these bonds: Asn417, Ser494, Ser496, Arg403, Arg408, and His505. The complex ZINC000008662732—spike (S1) had the second highest number of hydrogen bonds (total = 25847 hydrogen bonds), with an average of 259 bonds per nanosecond, followed by the ZINC000003995616—spike (S1) complex (total = 21750, mean = 218) and finally the ZINC000004098448—spike (S1) complex (total = 8607, mean = 86). In the case of the remdesivir-spike protein complex (Figure 4C), there was a formation of 6074 hydrogen bonds in the entire period of molecular dynamics, and the RBD amino acids and three RBD amino acid residues (Ser494, Ser496, Arg408) were identified that were also involved in the binding with our four ligands.

3.3. Calculation of free energies MM/PBSA and MM/GBSA

Table 4 shows the summary calculation of the average MM/PBSA and MM/GBSA binding free energies of the ΔG

Table 2. Comparison of spike protein (RBD)-ligand complex interactions from virtual screening and molecular docking analyzes.

Modeling	Compound ID	RBD amino acids involved in the interaction	Type of interaction
Virtual screening (PyRx)	ZINC000045789238	Ser496, Thr500, His505	Hydrogen bond
	ZINC000003995616	Ser496, Tyr495, Tyr501	carbon-hydrogen bond, pi-alkyl and pi-pi-shaped
	ZINC000004098448	Asn477, Lys478, Ala484, Phe486	pi-alkyl, pi-pi-shaped, and carbon-hydrogen bond
	ZINC000008662732	Arg408, Asn417, Tyr453	Hydrogen bond and carbon-hydrogen bond
Molecular docking (Autodock tools)	ZINC000045789238	Ser494, Ser496, Thr500, Thr501, His505	Hydrogen bond
	ZINC000003995616	Asp405, Ser496, Tyr495, Tyr501,	Hydrogen bond, attractive charge, pi-alkyl, carbon-hydrogen bond, and pi-pi-shaped
	ZINC000004098448	Lys478, Val483, Phe486	pi-alkyl, pi-pi T shaped
	ZINC000008662732	Arg403, Arg408, Gln409, Asn417, Tyr453, Ser496, His505,	Hydrogen bond, carbon-hydrogen bond
Molecular docking (Autodock Vina)	ZINC000045789238	Ser496, Thr500, Thr501	Hydrogen bond
	ZINC000003995616	Ser496, Tyr495, Tyr501	carbon-hydrogen bond, pi-alkyl and pi-pi-shaped
	ZINC000004098448	Lys478, Phe486, Val483	pi-alkyl, pi-pi-shaped, and carbon-hydrogen bond
	ZINC000008662732	Arg408, Tyr453, His505	Hydrogen bond and carbon-hydrogen bond

Naringenin-4′-O-Glucuronide (ZINC000045789238), ergoloid (ZINC000003995616), ohioensin A (ZINC000004098448) and prunetrin (ZINC000008662732).

Table 3. Docking results using two different exhaustiveness values (16 and 100) of the top 4 ligands with the highest affinity for SARS-CoV-2 RBD.

Compound ID	RBD amino acids involved in the interaction	Type of interaction	RBD amino acids involved in the interaction	Type of interaction
ZINC000045789238	Ser494, Ser496, Thr500, Tyr501, His505	Hydrogen bond	Arg403, Arg498, Ser496, Thr500, Tyr501, His505	Hydrogen bond, carbon-hydrogen bond, pi-pi T-shaped and pi-pi-stacked
ZINC000003995616	Asp405, Tyr495, Ser496, Tyr501	Hydrogen bond, attractive charge, pi-alkyl, carbon-hydrogen bond, pi-pi-shaped,	Asp405, Tyr495, Ser496, Tyr501, His505	Hydrogen bond, attractive charge, pi-alkyl, carbon-hydrogen bond, pi-pi stacked and pi-pi T-shaped
ZINC000004098448	Lys478, Val483, Phe486	pi-alkyl, pi-pi T shaped	Lys478, Val483, Phe486	pi-alkyl, pi-pi T shaped
ZINC000008662732	Arg403, Arg408, Gln409, Asn417, Tyr453, Ser496, His505,	Hydrogen bond, carbon-hydrogen bond	Arg403, Arg408, Gln409, Asn417, Tyr453, Ser496, His505	Hydrogen bond, carbon-hydrogen bond, Pi-cation, pi-pi stacked
Remdesivir	———	———	Arg403, Glu406, Gln409, Thr415, Asn417, Tyr453, Leu455, Tyr495, Phe497, Tyr501, His505	attractive charge, Hydrogen bond, carbon-hydrogen, Pi-sigma, alkyl, and pi-alkyl

Naringenin-4′-O-Glucuronide (ZINC000045789238), ergoloid (ZINC000003995616), ohioensin A (ZINC000004098448) and prunetrin (ZINC000008662732).

Complex, ΔG Receptor (spike protein), and ΔG Ligand, as well as the energy difference ΔG (Complex - Receptor—Ligand). All four ligands had a mean (-) MM/GBSA values for the ΔG complex and the ΔG difference (Complex - Receptor—Ligand). However, only the ligand ZINC000045789238 had a (-) average MM/GBSA binding free energy for the ΔG (Complex - Receptor –Ligand), which was − 3.74 kcal/mol, meaning that this complex was the only one to establish a bond with favorable energy to the molecular target. The remaining three ligands had (+) average MM/PBSA. The MM/PBSA and MM/GBSA results of remdesivir are similar to those found by our promising molecule (naringenin-4′-O-glucuronide), that is, MM/PBSA and MM/GBSA values less than zero (Table 4). Such similarity consolidates our results that suggest that the phytochemical naringenin-4′-O-glucuronide is a potential drug candidate for the treatment of COVID-19.

Figure 5 shows the results of the post-molecular dynamics (post-MD) simulation calculations. We can observe that the result of the calculations of the distances (Å) of the center of masses (CoM) per frame shown in Figure 5A, the ZINC000045789238-spike complex was the only one with smaller CoM distances. Its profile of CoM is similar to the CoM profile of the remdesivir-spike complex (control drug) at every post-MD simulation time. Calculations of MM/GBSA binding free energies per frame (Figure 5C), all four ligands tested, and remdesivir (control drug) showed good binding stability [(-) (MM/GBSA]. However, for the calculation of free energy of MM/PBSA binding per frame (Figure 5B), only the ligand ZINC000045789238 and remdesivir (control drug) were the ones that presented free energy of stable binding with the Spike protein of SARS-CoV-2 [(-) (MM/PBSA].

According to the predictions made on the ADMETLAB2 platform (Table 5), all four compounds evaluated (naringenin-4′-O-glucuronide, Ohioensin A, prunetrin, and ergoloid) had drug-like characteristics according to Pfizer's rule and golden triangle. Table 4 shows the results of the predictions of the pharmacokinetic parameters. Of the four compounds,

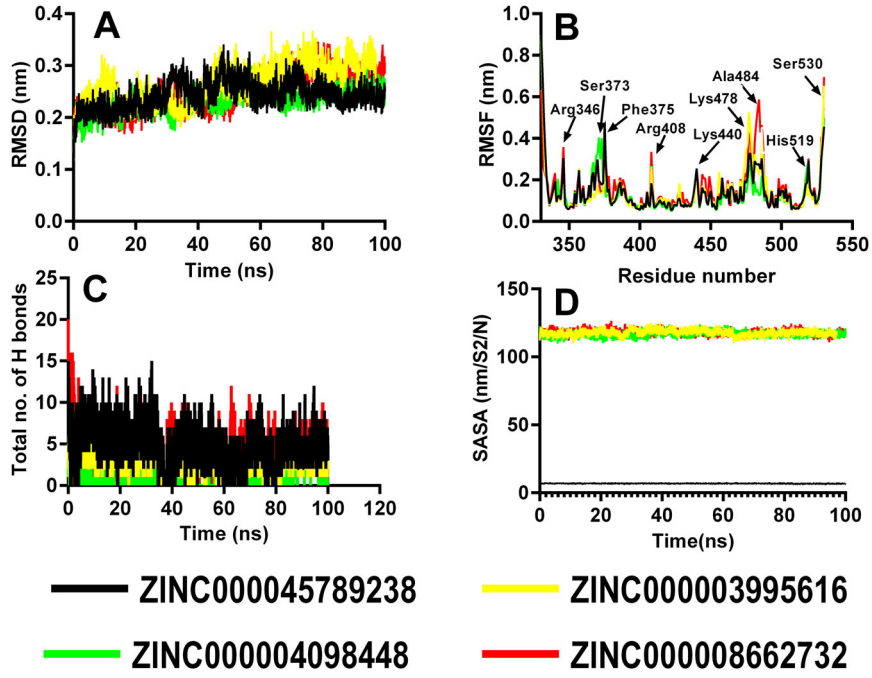

Figure 3. Molecular dynamics simulations of the top four ligands. Figures A, B, C, and D show the profile of RMSD, RMSF, total hydrogen bonding, and solvent accessibility for the molecular dynamics simulations at a time of 100 ns. The complexes naringenin-4′-O-Glucuronide (ZINC000045789238)-spike, ergoloid (ZINC000003995616)-spike, ohioensin A (ZINC000004098448)-spike, and prunetrin (ZINC000008662732)-spike are colored in black, yellow, green and red, respectively.

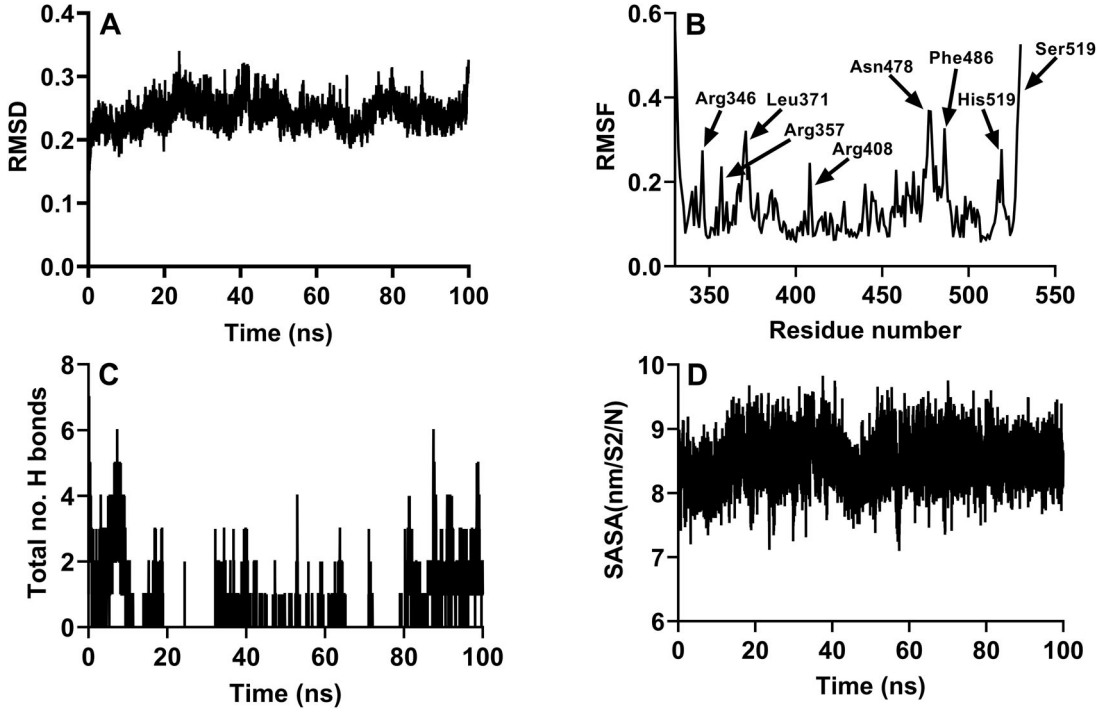

Figure 4. Molecular dynamics simulations of remdesivir (reference drug). Figures A, B, C, and D show the profile of RMSD, RMSF, total hydrogen bonding, and solvent accessibility for the molecular dynamics simulations at a time of 100 ns.

only naringenin-4′-O-glucuronide and ohioensin A had a higher likelihood of oral and increased absorption and good bioavailability. However, in the distribution, only naringenin-4′-O-glucuronide had the four distribution parameters (Plasma Protein Binding, Volume Distribution, Blood–Brain Barrier, and FU) simultaneously within the acceptable range values. Naringenin-4′-O-glucuronide was shown to be more likely to be a CYP2C9 substrate. At elimination, all four molecules had clearance values within the tolerated range.

Table 6 shows the results of the acute and chronic toxicity predictions that were obtained on the PROTOX II platform. Among the four analyzed compounds, only the ohioensin A ligand was the one that presented some type of toxicity (cytotoxicity, ER, ER-LBD, MMP, and Phosphoprotein p53). In

Table 4. MM/PBSA and MM/GBSA binding free energy of spike protein (S1) and ligand complex.

			MM/PBSA	
ZINC ID (ligand)	ΔG Complex	ΔG Receptor	ΔG Ligand	ΔG (Complex - Receptor –Ligand)
ZINC000045789238	−1983.33	−1993.60	14.01	−3.74
ZINC000004098448	−1961.07	−2010.66	47.64	1.95
ZINC000008662732	−1875.03	−1989.50	106.42	8.04
ZINC000003995616	−1933.84	−2003.13	63.19	6.11
Remdesivir	−1721.55	−1919.07	202.82	−5.30
			MM/GBSA	
ZINC ID (ligand)	ΔG Complex	ΔG Receptor	ΔG Ligand	ΔG (Complex - Receptor –Ligand)
ZINC000045789238	−2539.84	−2543.37	19.18	−15.65
ZINC000004098448	−2522.03	−2562.51	51.83	−11.35
ZINC000008662732	−2428.50	−2532.94	112.70	−8.25
ZINC000003995616	−2496.10	−2549.13	66.14	−13.10
Remdesivir	−2276.65	−2469.59	201.68	−8.73

Note: Naringenin-4′-O-Glucuronide (ZINC000045789238), ergoloid (ZINC000003995616), ohioensin A (ZINC000004098448) and prunetrin (ZINC000008662732).

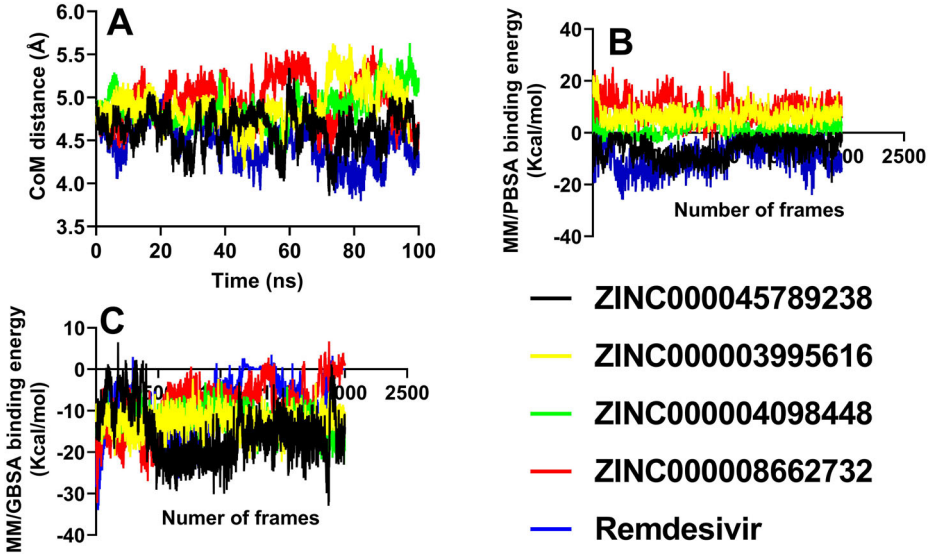

Figure 5. Post-molecular dynamics (Post-MD) simulations of the top four ligands and rendesivir (control drug). Figures A, B, and C show the profile of the center of mass (CoM) per frame, binding free energy MM/PBSA per frame, and binding free energy MM/GBSA per frame for the post-MD simulations at a time of 20 ns. The complexes naringenin-4′-O-Glucuronide (ZINC000045789238)-spike, ergoloid (ZINC000003995616)-spike, ohioensin A (ZINC000004098448)-spike, prunetrin (ZINC000008662732)-spike and remdesivir-spike are colored in black, yellow, green, red and blue, respectively.

Table 5. Prediction of pharmacokinetic parameters of the top four ligands that had the highest affinity for the spike protein (S1) RBD of the omicron mutation.

	Naringenin-4′-O-glucuronide	Ohioensin A	Prunetrin	Ergoloid	
Pharmacokinetic parameter	Probability/Value*	Probability/Value*	Probability/Value*	Probability/Value*	Observation
Absorption					
Human Intestinal Absorption (%)	70-90	70-90	0.0-10	0.0-10	————————
F (20% Bioavailability) (%)	70-90	70-90	10-30	0.0-10	————————
Distribution					
Plasma Protein Binding (%)	87.12	92.757	87.730	93.306	Optimal: < 90
Volume Distribution (L/kg)	0.37	1.857	0.741	3.095	Optimal: 0.04 – 20
Blood–Brain Barrier (%)	0.0-10	0.0-10	8.802	30-50	
FU (%)	12.89	4.387		3.056	Low < 5; Midle:5-20; High > 20
Metabolism					
CYP1A2 inhibitor (%)	0.0-10	10-30	30-50	0.0-10	————————
CYP1A2 substrate (%)	0.0-10	70-90	10-30	0.0-10	————————
CYP2C19 inhibitor (%)	0.0-10	10-30	0.0-10	50-70	————————
CYP2C19 substrate (%)	0.0-10	90-100	0.0-10	90-100	————————
CYP2C9 inhibitor (%)	0.0-10	0.0-10	10-30	90-100	————————
CYP2C9 substrate (%)	70 – 90	10-30	70 – 90	10-30	————————
CYP2D6 inhibitor (%)	0.0-10	0.0-10	30-50	0.0-10	————————
CYP2D6 substrate (%)	0.0-10	10-30	30-50	10-30	————————
CYP3A4 inhibitor (%)	0.0-10	10-30	10-30	90-100	————————
CYP3A4 substrate (%)	0.0-10	90-100	0.0-10	90-100	————————
Excretion					
Clearance Rate (mL/min/kg)	5.295	6.145	5.987	14.675	Low < 5; Midle:5-15; High > 15
Half Life Time (h)	0.808	0.165	0.586	0.727	Short < 3; Long > 3

*For the classification endpoints, the prediction probability values are transformed into six symbols: 0-10% (- - -), 10-30% (- -), 30-50% (-), 50-70% (+), 70-90% (+ +), and 90-100% (+ + +).

Table 6. Prediction of acute and chronic toxicity of the top four ligands that had the highest affinity for the spike protein (S1) RBD of the Omicron mutation.

Type of toxicity	Naringenin-4′-O-glucuronide		Ohioensin A		Prunetrin		Ergoloid	
	Prediction	Probability	Prediction	Probability	Prediction	Probability	Prediction	Probability
Hepatotoxicity	Inactive	0.74	Inactive	0.71	Inactive	0.83	Inactive	0.96
Carcinogenicity	Inactive	0.60	Inactive	0.58	Inactive	0.90	Inactive	0.52
Mutagenicity	Inactive	0.68	Inactive	0.62	Inactive	0.65	Inactive	0.90
Cytotoxicity	Inactive	0.84	**Active**	0.68	Inactive	0.58	Inactive	0.54
AhR	Inactive	0.81	Inactive	0.59	Inactive	0.62	Inactive	0.99
Androgen Receptor	Inactive	0.98	Inactive	0.91	Inactive	0.98	Inactive	0.99
AR-LBD	Inactive	0.96	Inactive	0.95	Inactive	1.0	Inactive	1.0
Aromatase	Inactive	0.96	Inactive	0.79	Inactive	0.99	Inactive	0.94
ER	Inactive	0.86	**Active**	0.65	Inactive	0.97	Inactive	0.98
ER-LBD	Inactive	0.93	**Active**	0.52	Inactive	0.99	Inactive	1.0
PPAR-Gamma	Inactive	0.91	Inactive	0.62	Inactive	0.99	Inactive	0.98
nrf2/ARE	Inactive	0.90	Inactive	0.91	Inactive	0.99	Inactive	0.93
HSE	Inactive	0.90	Inactive	0.91	Inactive	0.99	Inactive	0.93
MMP	Inactive	0.65	**Active**	0.72	Inactive	0.99	Inactive	0.86
Phosphoprotein p53	Inactive	0.80	**Active**	0.55	Inactive	0.86	Inactive	0.98
ATAD5	Inactive	0.94	Inactive	0.75	Inactive	0.99	Inactive	0.99
Acute toxicity (LD50)	2300 mg/kg		2000 mg/kg		5000 mg/kg		2000 mg/kg	

Aryl hydrocarbon Receptor (AhR); Androgen Receptor Ligand Binding Domain (AR-LBD); Estrogen Receptor Alpha (ER); Estrogen Receptor Ligand Binding Domain (ER-LBD); Peroxisome Proliferator Activated Receptor Gamma (PPAR-Gamma); Nuclear factor (erythroid-derived 2)-like 2/antioxidant responsive element (nrf2/ARE); Heat shock factor response element (HSE); Mitochondrial Membrane Potential (MMP); ATPase family AAA domain-containing protein 5 (ATAD5).

contrast, the rest of the three ligands showed no kind of toxicity. The results of acute toxicity showed that all compounds had a lethal dose greater than 2000 mg/kg and were classified as compounds of class V toxicity, which is the class of compounds unlikely to cause acute damage.

4. Discussion

This study evaluated more than 170,000 NBCs as potential alternatives against COVID-19 using docking and MD simulations, including MM/PBSA and MM/GBSA trials. Although we initially identified four compounds (Table 1) as having a higher binding affinity with the spike (S1) protein of the Omicron variant of the virus, only the chemical compound naringenin-4′-O-glucuronide (ID ZINC000045789238) presented promising results during the MD simulations.

The Omicron variant of SARS-Cov-2 is currently a significant concern in the fight against COVID-19, given its mutational patterns (Chekol Abebe et al., 2022; Rahmani & Rezaei, 2022). It is known that the spike protein (S1), specifically the RBD region, is responsible for the virus's recognition of the host cells (human ACE-2) (Kannan et al., 2021; Tian et al., 2022). In the case of the spike protein (S1) of the Omicron variant, several mutations of the amino acid residues of the RBD region have been reported (Asp339, Asp339, Pro373, Phe375, Asn417, Lys440, Ser446, Asn477, Lys478, Ala484, Arg493, Ser496, Ar498, TyR501, and His505) (Brüssow & Brüssow, 2022; Mannar et al., 2022). Besides providing a higher speed of dissemination to the virus, these mutations challenge the development or improvement of vaccines and treatments that can increase individuals' immunity (Ao et al., 2022; Fan et al., 2022). There is also scientific evidence showing several cases of re-infection by Omicron, thus requiring the administration of booster vaccines (Fan et al., 2022).

Several docking studies and molecular dynamics simulations aimed at identifying new inhibitors against different target proteins of SARS-CoV-2 are available in the literature (Badavath et al., 2022; Fayyazi et al., 2022; Sen et al., 2022; Sen Gupta et al., 2022; Thakur et al., 2022). For example, Gangadevi et al. (2021) identified kobophenol A as a potential inhibitor of the Spike protein RBD (S1), where the amino acids Glu375 and Thr347 established hydrogen bonds with the spike protein (Gangadevi et al., 2021). Two possible reasons explain the differences in the amino acid residues involved in the interaction of the protein-ligand complex between our study and the study by Gangadevi et al. (2021): first, because Gangadevi et al. (2021) used the spike protein from the SARS-CoV-2 wild types (PDB ID 6M0J) (Lan et al., 2020), unlike our study where we used the spike protein of SARS-CoV-2 that underwent omicron mutation (PDB ID 7T9L) (Mannar et al., 2022). The following explanation is that in the study by Gangadevi et al. (2021), the docking and molecular dynamics of the ligands were done with the RBD/ACE-2 spike complex. The ligands were linked in a different site of the RBD (Gangadevi et al., 2021). In contrast, in our study, we isolated the ACE-2 spike protein and sought to investigate ligands that inhibit specific RBD amino acids involved in ACE-2 binding (Asp339, Asp339, Pro373, Phe375, Asn417, Lys440, Ser446, Asn477, Lys478, Ala484, Arg493, Ser496, Ar498, TyR501, and His505) (Mannar et al., 2022). On the other hand, the RBD amino acids identified in ours were also found in the study by Kumar et al. (2022), wherein molecular dynamics assays the drug favipiravir showed promising results in inhibiting the RBD of the Spike protein of SARS-CoV-2 blocking amino acids Arg408 (HB), Gln409 (hydrophobic) by hydrogen bonding and hydrophobic interactions, respectively (Kumar et al., 2022). Also, in the study by Kumar et al. (2022), isochlorogenic acid had a greater binding affinity with the amino acids Tyr453 and Tyr453 of RBD *via* hydrogen bonds (Kumar et al., 2022).

We would also like to point out that we performed molecular docking analyses and molecular dynamics simulations using remdesivir as a reference drug, and the results found were similar to those found by our four promising ligands (Naringenin-4′-O-Glucuronide, ergoloid ohioensin A and prunetrin).

One way to ensure the reliability and accuracy of docking results is to perform consensual docking using different software (Poli et al., 2016; Tuccinardi et al., 2014). Using three different software (PyRx, AutoDock tools, and AutoDockVina), we could provide reliable results, with reported binding energy values of the top four ligands <2%. A total of nine conformations (poses) were generated, and we selected the one with the highest binding stability (*i.e.*, RMSD values <2.0), which reveals the accuracy of the docking results.

Non-covalent interactions such as hydrogen bonds play an essential role in recognizing the ligand to the molecular target and stabilizing the binding of the target-ligand complex (Gancia et al., 2001). In addition, many quantitative structure-activity relationships (QSAR) studies demonstrate that hydrogen bonds are essential in modeling a specific target activity (Fujita et al., 1977). In our study, the analysis of docking interactions showed that the ligand naringenin-4′-O-glucuronide (ID ZINC000045789238) produced the highest number of hydrogen bonds ($n = 6$) with amino acid residues in the RBD region of the spike protein (S1) of the Omicron mutation (Ser494, Ser496, Thr500, Thr5051, and Thr505). Prunetrin (ID ZINC000008662732) was the ligand with the second-highest number of hydrogen bonds (Arg408, Asp417, Ser496, and His505).

A plot of RMSD versus simulation time is commonly used to establish the ligand-target molecular complex's equilibrium period, stability, and binding quality in MD analyses. Overall, in our study, all four ligands formed a ligand-protein complex with mean RMSD values lower than 0.3 nm throughout the dynamics time of 100 ns, which is considered acceptable (da Fonseca et al., 2022; Kozakov et al., 2005; Mukherjee et al., 2010; Shoichet & Kuntz, 1991; Wright et al., 2013).

The RMSF is used to analyze the fluctuation (or stability) of atoms (or groups of atoms) of the apo-ligand receptor complex and the protein-ligand complexes in general, as can be observed in some studies in the literature involving the RBD complex of the protein spike of SARS-CoV-2 and ligands (Kalathiya et al., 2021; Sabzian-Molaei et al., 2022; Taka et al., 2021). In our study, RMSF values were also determined to understand the stability/fluctuations of the four complexes (Jamroz et al., 2014; Vardhan & Sahoo, 2020). Although all amino acid residues of the spike glycoprotein (S1) showed fluctuations within the tolerated limit (RMSF < 1.3 nm), as expected (Ahmed et al., 2021), the residues of the Omicron mutation involved in the interaction with the ligand (Phe375, Lys440, Lys478, and Phe375) presented important fluctuations. Previous studies have shown that these mutant residues are responsible for dynamic order-disorder transitions during the binding of the spike protein (S1) with human ACE-2, which may explain the figures obtained in our analyses (S. Kumar et al., 2022; Mannar et al., 2022).

In our study, all four complexes had stability in solvent accessibility and compatibility with the protein-ligand complex throughout the dynamic simulation period (100 ns) (Ahmed et al., 2021), as demonstrated in the SASA graph. The naringenin-4′-O-glucuronide-spike(S1) complex had the highest number of hydrogen bonds whose results correlate to those from the docking analyses.

MM/PBSA and MM/GBSA are two methods popularly used in MD simulations because they have high precision in the calculation of the free energy of binding between a ligand and molecular target in the whole trajectory of MD, being strongly recommended by scientists in the field (Genheden & Ryde, 2015). In our analyses, only the naringenin-4′-O-glucuronide–spike (S1) complex had (-) results for MM/PBSA and MM/GBSA binding free energies, showing greater binding stability with the spike protein (S1) and, therefore, being a promising drug candidate against SARS-CoV-2 infections. Conversely, although the remaining ligands, ZINC000003995616, ZINC000004098448, and ZINC000008662732, had acceptable dynamic equilibrium values (RMSD < 0.3 nm), they should not be considered drug candidates for this indication due to the lack of spike protein binding stability (MM/PBSA > 0).

Naringenin is a phytochemical of the class of flavonoids known to have potent antiviral and immunomodulatory activity, including against the SARS-Cov-2 virus (Tutunchi et al., 2020; Zeng et al., 2018). However, no studies were found in the literature concerning activity against SARS-Cov-2 for the compound naringenin-4′-O-glucuronide identified in our research. However, since naringenin-4′-O-glucuronide is a naringenin derivative, it likely has an action against SARS-Cov-2. *In vitro* and *in vivo* studies are needed to consolidate our findings.

The high computational cost in performing MD simulations was the main limitation of this study. Although we used 100 ns for the MD simulations, as usually recommended in the literature (Majumder & Mandal, 2022; Mishra et al., 2021; Rashdan & Abdelmonsef, 2022; Sepay et al., 2021), we acknowledge that an increase in MD time could generate further information, such as protein folding and secondary structure behavior (alpha helix and beta-pleated sheets).

5. Conclusion

Using docking techniques, drug-likeness calculations, ADMET predictions, MD and post-MD simulations, we virtually screened over 170,000 natural compounds against the spike protein (S1) RBD of the Omicron variant of COVID-19. In the docking calculations, we identified four phytochemical molecules with the highest affinity for the RBD Spike protein (naringenin-4′-O-glucuronide, ergoloid, ohioensin A and prunetrin). However, in drug-likeness, ADMET, MD and post-MD calculations, naringenin-4′-O-glucuronide was the most promising compound for inhibiting the following mutant amino acid residues: Asn417, Ser494, Ser496, Arg403, Arg408, and His505. These results revealed naringenin-4′-O glucuronide as a potential drug candidate against COVID-19. Additionally, we recognize the importance of experimental validation suggested by the reviewers, but this would be the study's next step because the present study's objective is to investigate drug candidates against COVID-19 using in silico methods.

Acknowledgments

The authors express their gratitude to the Brazilian National Council of Technological and Scientific Development (CNPq) and CAPES (Brazilian

Federal Agency for Support and Evaluation of Graduate Education within the Ministry of Education of Brazil) for research funding – Finance Code 001

Disclosure statement

No potential conflict of interest was reported by the authors.

Funding

The author(s) reported there is no funding associated with the work featured in this article.

ORCID

Alexandre de Fátima Cobre http://orcid.org/0000-0001-6642-3928
Moisés Maia Neto http://orcid.org/0000-0002-9337-2043
Mariana Millan Fachi http://orcid.org/0000-0001-5918-4738
Luana Mota Ferreira http://orcid.org/0000-0001-9951-587X
Fernanda Stumpf Tonin http://orcid.org/0000-0003-4262-8608
Roberto Pontarolo http://orcid.org/0000-0002-7049-4363

Authors' contributions

Study concepts: AFC, RP, FST, MMN. Study design: AFC, FST, RP, DPS, MMN, EBM. Data acquisition: AFC, MMN, MMF. Statistical analysis: AFC, MMN, MMF.

Manuscript preparation: AFC, RP, FST, LMF. Manuscript editing: AFC, RP, EBM, FST, LMF. Manuscript review: AFC, RP, EBM, FST, LMF, MMF.

References

Ahmed, S., Mahtarin, R., Ahmed, S. S., Akter, S., Islam, M. S., Mamun, A. A., Islam, R., Hossain, M. N., Ali, M. A., Sultana, M. U. C., Parves, M. R., Ullah, M. O., & Halim, M. A. (2021). Investigating the binding affinity, interaction, and structure-activity-relationship of 76 prescription antiviral drugs targeting RdRp and Mpro of SARS-CoV-2. *Journal of Biomolecular Structure & Dynamics*, *39*(16), 6290–6305. https://doi.org/10.1080/07391102.2020.1796804

Allouche, A. R. (2011). Gabedit—A graphical user interface for computational chemistry softwares. *Journal of Computational Chemistry*, *32*(1), 174–182. https://doi.org/10.1002/JCC.21600

Alnajjar, R., Mostafa, A., Kandeil, A., & Al-Karmalawy, A. A. (2020). Molecular docking, molecular dynamics, and in vitro studies reveal the potential of angiotensin II receptor blockers to inhibit the COVID-19 main protease. *Heliyon*, *6*(12), e05641. https://doi.org/10.1016/j.heliyon.2020.e05641

Ao, D., Lan, T., He, X., Liu, J., Chen, L., Baptista-Hon, D. T., Zhang, K., & Wei, X. (2022). SARS-CoV-2 Omicron variant: Immune escape and vaccine development. *MedComm*, *3*(1), e126. https://doi.org/10.1002/MCO2.126

Badavath, V. N., Kumar, A., Samanta, P. K., Maji, S., Das, A., Blum, G., Jha, A., & Sen, A. (2022). Determination of potential inhibitors based on isatin derivatives against SARS-CoV-2 main protease (mpro): A molecular docking, molecular dynamics and structure-activity relationship studies. *Journal of Biomolecular Structure & Dynamics*, *40*(7), 3110–3128. https://doi.org/10.1080/07391102.2020.1845800

Banerjee, P., Eckert, A. O., Schrey, A. K., & Preissner, R. (2018). ProTox-II: A webserver for the prediction of toxicity of chemicals. *Nucleic Acids Research*, *46*(W1), W257–W263. https://doi.org/10.1093/NAR/GKY318

Berman, H., Henrick, K., Nakamura, H., & Markley, J. L. (2007). The worldwide Protein Data Bank (wwPDB): ensuring a single, uniform archive of PDB data. *Nucleic Acids Research*, *35*(Database issue), D301–D303. https://doi.org/10.1093/NAR/GKL971

Brüssow, H., & Brüssow, B. (2022). COVID-19: Omicron – the latest, the least virulent, but probably not the last variant of concern of SARS-CoV-2. *Microbial Biotechnology*, *15*(7), 1927–1939. https://doi.org/10.1111/1751-7915.14064

Cao, Y., Wang, J., Jian, F., Xiao, T., Song, W., Yisimayi, A., Huang, W., Li, Q., Wang, P., An, R., Wang, J., Wang, Y., Niu, X., Yang, S., Liang, H., Sun, H., Li, T., Yu, Y., Cui, Q., … Xie, X. S. (2022). Omicron escapes the majority of existing SARS-CoV-2 neutralizing antibodies. *Nature*, *602*(7898), 657–663. https://doi.org/10.1038/s41586-021-04385-3

Cheatham, T. E., Miller, J. L., Fox, T., Darden, T. A., & Kollman, P. A. (1995). Molecular dynamics simulations on solvated biomolecular systems: The particle mesh Ewald method leads to stable trajectories of DNA, RNA, and proteins. *Journal of the American Chemical Society*, *117*(14), 4193–4194. https://doi.org/10.1021/JA00119A045/ASSET/JA00119A045.FP.PNG_V03

Chekol Abebe, E., Medhin, M. T. G., Mariam, A. B. T., Dejenie, T. A., Ayele, T. M., Admasu, F. T., Muche, Z. T., & Adela, G. A. (2022). Mutational pattern, impacts and potential preventive strategies of omicron SARS-CoV-2 variant infection. *Infection and Drug Resistance*, *15*, 1871–1887. https://doi.org/10.2147/IDR.S360103

Cuzzolin, A., Sturlese, M., Malvacio, I., Ciancetta, A., & Moro, S. (2015). DockBench: An integrated informatic platform bridging the gap between the robust validation of docking protocols and virtual screening simulations. *Molecules (Basel, Switzerland)*, *20*(6), 9977–9993. https://doi.org/10.3390/MOLECULES20069977

da Fonseca, A. M., Soares, N. B., Meirú, M. I. L., Colares, R. P., Neto, M. M., Sobrinho, A. C. N., dos Santos, H. S., & Marinho, E. S. (2022). Combined study of docking and molecular dynamics against DNV-3 SN1 protein by bixinoids. https://doi.org/10.1080/07391102.2022.2070282

Dallakyan, S., & Olson, A. J. (2015). Small-molecule library screening by docking with PyRx. *Methods in Molecular Biology*, *1263*, 243–250. https://doi.org/10.1007/978-1-4939-2269-7_19

Elsbaey, M., Ibrahim, M. A. A., Bar, F. A., & Elgazar, A. A. (2021). Chemical constituents from coconut waste and their in silico evaluation as potential antiviral agents against SARS-CoV-2. *South African Journal of Botany: Official Journal of the South African Association of Botanists = Suid-Afrikaanse Tydskrif Vir Plantkunde: Amptelike Tydskrif Van Die Suid-Afrikaanse Genootskap Van Plantkundiges*, *141*, 278–289. https://doi.org/10.1016/J.SAJB.2021.05.018

Fan, Y., Li, X., Zhang, L., Wan, S., Zhang, L., & Zhou, F. (2022). SARS-CoV-2 Omicron variant: Recent progress and future perspectives. *Signal Transduction and Targeted Therapy*, *7*(1), 1–11. https://doi.org/10.1038/s41392-022-00997-x

Fayyazi, N., Mostashari-Rad, T., Ghasemi, J. B., Ardakani, M. M., & Kobarfard, F. (2022). Molecular dynamics simulation, 3D-pharmacophore and scaffold hopping analysis in the design of multi-target drugs to inhibit potential targets of COVID-19. *Journal of Biomolecular Structure & Dynamics*, *40*(22), 11787–11808. https://doi.org/10.1080/07391102.2021.1965914

Field, M. J., Albe, M., Bret, C., Martin, P.-D., & Thomas, A. (2000). The dynamo library for molecular simulations using hybrid quantum mechanical and molecular mechanical potentials. *Journal of Computational Chemistry*, *21*(12), 1088–1100. https://doi.org/10.1002/1096-987X

Fujita, T., Nishioka, T., & Nakajima, M. (1977). Hydrogen-bonding parameter and its significance in quantitative structure-activity studies. *Journal of Medicinal Chemistry*, *20*(8), 1071–1081. https://doi.org/10.1021/JM00218A017/ASSET/JM00218A017.FP.PNG_V03

Gancia, E., Montana, J. G., & Manallack, D. T. (2001). Theoretical hydrogen bonding parameters for drug design. *Journal of Molecular Graphics & Modelling*, *19*(3-4), 349–362. https://doi.org/10.1016/S1093-3263(00)00084-X

Gangadevi, S., Badavath, V. N., Thakur, A., Yin, N., De Jonghe, S., Acevedo, O., Jochmans, D., Leyssen, P., Wang, K., Neyts, J., Yujie, T., & Blum, G. (2021). Kobophenol A inhibits binding of host ACE2 receptor with spike RBD domain of SARS-CoV-2, a lead compound for blocking COVID-19. *The Journal of Physical Chemistry Letters*, *12*(7), 1793–1802. https://doi.org/10.1021/acs.jpclett.0c03119

Gasteiger, J., & Marsili, M. (1980). Iterative partial equalization of orbital electronegativity—a rapid access to atomic charges. *Tetrahedron*, *36*(22), 3219–3228. https://doi.org/10.1016/0040-4020(80)80168-2

Genheden, S., & Ryde, U. (2015). The MM/PBSA and MM/GBSA methods to estimate ligand-binding affinities. *Expert Opinion on Drug Discovery*, *10*(5), 449–461. https://doi.org/10.1517/17460441.2015.1032936

Hess, B., Bekker, H., Berendsen, H. J. C., & Fraaije, J. G. E. M. (1997). LINCS: A Linear Constraint Solver for Molecular Simulations. *Journal of Computational Chemistry*, *18*(12), 1463–1472. https://doi.org/10.1002/(SICI)1096-987X(199709)18:12

Hosseini, F. S., & Amanlou, M. (2020). Anti-HCV and anti-malaria agent, potential candidates to repurpose for coronavirus infection: Virtual screening, molecular docking, and molecular dynamics simulation study. *Life Sciences*, *258*, 118205. https://doi.org/10.1016/J.LFS.2020.118205

Humphrey, W., Dalke, A., & Schulten, K. (1996). VMD: Visual molecular dynamics. *Journal of Molecular Graphics*, *14*(1), 33–38. https://doi.org/10.1016/0263-7855(96)00018-5

Irwin, J. J., & Shoichet, B. K. (2005). ZINC-A free database of commercially available compounds for virtual screening. *Journal of Chemical Information and Modeling* *45*(1):177–182. https://doi.org/10.1021/CI049714

Islam, M. S., Mahmud, S., Sultana, R., & Dong, W. (2020). Identification and in silico molecular modelling study of newly isolated Bacillus subtilis SI-18 strain against S9 protein of Rhizoctonia solani. *Arabian Journal of Chemistry*, *13*(12), 8600–8612. https://doi.org/10.1016/j.arabjc.2020.09.044

Jamroz, M., Kolinski, A., & Kmiecik, S. (2014). CABS-flex predictions of protein flexibility compared with NMR ensembles. *Bioinformatics (Oxford, England)*, *30*(15), 2150–2154. https://doi.org/10.1093/BIOINFORMATICS/BTU184

Kalathiya, U., Padariya, M., Fahraeus, R., Chakraborti, S., & Hupp, T. R. (2021). Multivalent display of SARS-CoV-2 spike (RBD domain) of COVID-19 to nanomaterial, protein ferritin nanocages. *Biomolecules*, *11*(2), 297. https://doi.org/10.3390/biom11020297

Kannan, S., Shaik Syed Ali, P., & Sheeza, A. (2021). Omicron (B.1.1.529) - variant of concern - molecular profile and epidemiology: A mini review. *European Review for Medical and Pharmacological Sciences*, *25*(24), 8019–8022. https://doi.org/10.26355/EURREV_202112_27653

Kirchmair, J., Markt, P., Distinto, S., Wolber, G., & Langer, T. (2008). Evaluation of the performance of 3D virtual screening protocols: RMSD comparisons, enrichment assessments, and decoy selection–what can we learn from earlier mistakes? *Journal of Computer-Aided Molecular Design*, *22*(3–4), 213–228. https://doi.org/10.1007/S10822-007-9163-6

Kozakov, D., Clodfelter, K. H., Vajda, S., & Camacho, C. J. (2005). Optimal clustering for detecting near-native conformations in protein docking. *Biophysical Journal*, *89*(2), 867–875. https://doi.org/10.1529/BIOPHYSJ.104.058768

Kumar, B. H., Manandhar, S., Mehta, C. H., Nayak, U. Y., & Pai, K. S. R. (2022). Structure-based docking, pharmacokinetic evaluation, and molecular dynamics-guided evaluation of traditional formulation against SARS-CoV-2 spike protein receptor bind domain and ACE2 receptor complex. *Chemicke Zvesti*, *76*(2), 1063–1083. https://doi.org/10.1007/s11696-021-01917-z

Kumar, Y., Singh, H., & Patel, C. N. (2020). In silico prediction of potential inhibitors for the main protease of SARS-CoV-2 using molecular docking and dynamics simulation based drug-repurposing. *Journal of Infection and Public Health*, *13*(9), 1210–1223. https://doi.org/10.1016/J.JIPH.2020.06.016

Lan, J., Ge, J., Yu, J., Shan, S., Zhou, H., Fan, S., Zhang, Q., Shi, X., Wang, Q., Zhang, L., & Wang, X. (2020). Structure of the SARS-CoV-2 spike receptor-binding domain bound to the ACE2 receptor. *Nature*, *581*(7807), 215–220. https://doi.org/10.1038/S41586-020-2180-5

Liu, Y. (2023). Integrative network pharmacology and in silico analyses identify the anti-omicron SARS-CoV-2 potential of eugenol. *Heliyon*, *9*(3), e13853. https://doi.org/10.1016/j.heliyon.2023.e13853

Liu, L., Iketani, S., Guo, Y., Chan, J. F.-W., Wang, M., Liu, L., Luo, Y., Chu, H., Huang, Y., Nair, M. S., Yu, J., Chik, K. K.-H., Yuen, T. T.-T., Yoon, C., To, K. K.-W., Chen, H., Yin, M. T., Sobieszczyk, M. E., Huang, Y., … Ho, D. D. (2022). Striking antibody evasion manifested by the Omicron variant of SARS-CoV-2. *Nature*, *602*(7898), 676–681. https://doi.org/10.1038/s41586-021-04388-0

Majumder, R., & Mandal, M. (2022). Screening of plant-based natural compounds as a potential COVID-19 main protease inhibitor: An in silico docking and molecular dynamics simulation approach. *Journal of Biomolecular Structure & Dynamics*, *40*(2), 696–711. https://doi.org/10.1080/07391102.2020.1817787/SUPPL_FILE/TBSD_A_1817787_SM7020.PDF

Mannar, D., Saville, J. W., Zhu, X., Srivastava, S. S., Berezuk, A. M., Tuttle, K. S., Marquez, A. C., Sekirov, I., & Subramaniam, S. (2022). SARS-CoV-2 Omicron variant: Antibody evasion and cryo-EM structure of spike protein-ACE2 complex. *Science (New York, NY)*, *375*(6582), 760–764. https://doi.org/10.1126/SCIENCE.ABN7760

Mishra, D., Maurya, R. R., Kumar, K., Munjal, N. S., Bahadur, V., Sharma, S., Singh, P., & Bahadur, I. (2021). Structurally modified compounds of hydroxychloroquine, remdesivir and tetrahydrocannabinol against main protease of SARS-CoV-2, a possible hope for COVID-19: Docking and molecular dynamics simulation studies. *Journal of Molecular Liquids*, *335*, 116185. https://doi.org/10.1016/J.MOLLIQ.2021.116185

Mukherjee, S., Balius, T. E., & Rizzo, R. C. (2010). Docking validation resources: Protein family and ligand flexibility experiments. *Journal of Chemical Information and Modeling*, *50*(11), 1986–2000. https://doi.org/10.1021/CI1001982/SUPPL_FILE/CI1001982_SI_001.PDF

Oany, A. R., Mia, M., Pervin, T., Junaid, M., Hosen, S. M. Z., & Moni, M. A. (2020). Design of novel viral attachment inhibitors of the spike glycoprotein (S) of severe acute respiratory syndrome coronavirus-2 (SARS-CoV-2) through virtual screening and dynamics. *International Journal of Antimicrobial Agents*, *56*(6), 106177. https://doi.org/10.1016/J.IJANTIMICAG.2020.106177

O'Boyle, N. M., Banck, M., James, C. A., Morley, C., Vandermeersch, T., & Hutchison, G. R. (2011). Open Babel: An open chemical toolbox. *Journal of Cheminformatics*, *3*(33), 1-14. https://doi.org/10.1186/1758-2946-3-33

Pang, J., Gao, S., Sun, Z., & Yang, G. (2021). Discovery of small molecule PLpro inhibitor against COVID-19 using structure-based virtual screening, molecular dynamics simulation, and molecular mechanics/Generalized Born surface area (MM/GBSA) calculation. *Structural Chemistry*, *32*(2), 879–886. https://doi.org/10.1007/S11224-020-01665-Y

Phillips, J. C., Braun, R., Wang, W., Gumbart, J., Tajkhorshid, E., Villa, E., Chipot, C., Skeel, R. D., Kalé, L., & Schulten, K. (2005). Scalable molecular dynamics with NAMD. *Journal of Computational Chemistry*, *26*(16), 1781–1802. https://doi.org/10.1002/JCC.20289

Poli, G., Martinelli, A., & Tuccinardi, T. (2016). Reliability analysis and optimization of the consensus docking approach for the development of virtual screening studies. *Journal of Enzyme Inhibition and Medicinal Chemistry*, *31*(sup2), 167–173. https://doi.org/10.1080/14756366.2016.1193736/SUPPL_FILE/IENZ_A_1193736_SM2163.PDF

Rafi, M. O., Bhattacharje, G., Al-Khafaji, K., Taskin-Tok, T., Alfasane, M. A., Das, A. K., Parvez, M. A. K., & Rahman, M. S. (2022). Combination of QSAR, molecular docking, molecular dynamic simulation and MM-PBSA: Analogues of lopinavir and favipiravir as potential drug candidates against COVID-19. *Journal of Biomolecular Structure & Dynamics*, *40*(8), 3711–3730. https://doi.org/10.1080/07391102.2020.1850355/SUPPL_FILE/TBSD_A_1850355_SM5903.DOCX

Rahmani, S., & Rezaei, N. (2022). Omicron (B.1.1.529) variant: Development, dissemination, and dominance. *Journal of Medical Virology*, *94*(5), 1787–1788. https://doi.org/10.1002/JMV.27563

Rakib, A., Sami, S. A., Mimi, N. J., Chowdhury, M. M., Eva, T. A., Nainu, F., Paul, A., Shahriar, A., Tareq, A. M., Emon, N. U., Chakraborty, S., Shil, S., Mily, S. J., Ben Hadda, T., Almalki, F. A., & Emran, T. B. (2020). Immunoinformatics-guided design of an epitope-based vaccine against severe acute respiratory syndrome coronavirus 2 spike glycoprotein. *Computers in Biology and Medicine*, *124*, 103967. https://doi.org/10.1016/J.COMPBIOMED.2020.103967

Rashdan, H. R. M., & Abdelmonsef, A. H. (2022). In silico study to identify novel potential thiadiazole-based molecules as anti-Covid-19 candidates by hierarchical virtual screening and molecular dynamics simulations. *Structural Chemistry*, *33*(5), 1727–1739. https://doi.org/10.1007/S11224-022-01985-1/TABLES/3

Ravi, L., & Kannabiran, K. (2016). A handbook on protein-ligand docking tool: AutoDock4. *Innovare Journal of Medical Sciences*, *4*(3), 1-6.

https://www.researchgate.net/publication/304657251_A_Handbook_On_Protein-Ligand_Docking_Tool_AutoDock4

Sabzian-Molaei, F., Khalili, M. A. N., Sabzian-Molaei, M., Shahsavarani, H., Pour, A. F., Rad, A. M., & Hadi, A. (2022). Urtica dioica Agglutinin: A plant protein candidate for inhibition of SARS-COV-2 receptor-binding domain for control of Covid19 Infection. *Plos One*, *17*(7), e0268156. https://doi.org/10.1371/journal.pone.0268156

Sen Gupta, P. S., Biswal, S., Panda, S. K., Ray, A. K., & Rana, M. K. (2022). Binding mechanism and structural insights into the identified protein target of COVID-19 and importin-α with in-vitro effective drug ivermectin. *Journal of Biomolecular Structure & Dynamics*, *40*(5), 2217–2226. https://doi.org/10.1080/07391102.2020.1839564

Sen, D., Debnath, P., Debnath, B., Bhaumik, S., & Debnath, S. (2022). Identification of potential inhibitors of SARS-CoV-2 main protease and spike receptor from 10 important spices through structure-based virtual screening and molecular dynamic study. *Journal of Biomolecular Structure & Dynamics*, *40*(2), 941–962. https://doi.org/10.1080/07391102.2020.1819883

Sepay, N., Sekar, A., Halder, U. C., Alarifi, A., & Afzal, M. (2021). Anti-COVID-19 terpenoid from marine sources: A docking, admet and molecular dynamics study. *Journal of Molecular Structure*, *1228*, 129433. https://doi.org/10.1016/J.MOLSTRUC.2020.129433

Shoichet, B. K., & Kuntz, I. D. (1991). Protein docking and complementarity. *Journal of Molecular Biology*, *221*(1), 327–346. https://doi.org/10.1016/0022-2836(91)80222-G

Sterling, T., & Irwin, J. J. (2015). ZINC 15 - ligand discovery for everyone. *Journal of Chemical Information and Modeling*, *55*(11), 2324–2337. https://doi.org/10.1021/ACS.JCIM.5B00559/ASSET/IMAGES/LARGE/CI-2015-00559J_0005.JPEG

Sultana, J., Crisafulli, S., Gabbay, F., Lynn, E., Shakir, S., & Trifirò, G. (2020). Challenges for drug repurposing in the COVID-19 pandemic era. *Frontiers in Pharmacology*, *11*, 588654. https://doi.org/10.3389/FPHAR.2020.588654/BIBTEX

Taka, E., Yilmaz, S. Z., Golcuk, M., Kilinc, C., Aktas, U., Yildiz, A., & Gur, M. (2021). Critical interactions between the SARS-CoV-2 spike glycoprotein and the human ACE2 receptor. *The Journal of Physical Chemistry. B*, *125*(21), 5537–5548. https://doi.org/10.1021/ACS.JPCB.1C02048

Thakur, A., Sharma, G., Badavath, V. N., Jayaprakash, V., Merz, K. M., Blum, G., & Acevedo, O. (2022). Primer for designing main protease (Mpro) inhibitors of SARS-CoV-2. *The Journal of Physical Chemistry Letters*, *13*(25), 5776–5786. https://doi.org/10.1021/ACS.JPCLETT.2C01193

Tian, D., Sun, Y., Xu, H., & Ye, Q. (2022). The emergence and epidemic characteristics of the highly mutated SARS-CoV-2 Omicron variant. *Journal of Medical Virology*, *94*(6), 2376–2383. https://doi.org/10.1002/JMV.27643

Tingle, B. I., Tang, K. G., Castanon, M., Gutierrez, J. J., Khurelbaatar, M., Dandarchuluun, C., Moroz, Y. S., & Irwin, J. J. (2023). ZINC-22—a free multi-billion-scale database of tangible compounds for ligand discovery. *Journal of Chemical Information and Modeling*, *63*(4), 1166–1176. https://doi.org/10.1021/ACS.JCIM.2C01253/ASSET/IMAGES/LARGE/CI2C01253_0005.JPEG

Tuccinardi, T., Poli, G., Romboli, V., Giordano, A., & Martinelli, A. (2014). Extensive consensus docking evaluation for ligand pose prediction and virtual screening studies. *Journal of Chemical Information and Modeling*, *54*(10), 2980–2986. https://doi.org/10.1021/CI500424N/SUPPL_FILE/CI500424N_SI_001.PDF

Tutunchi, H., Naeini, F., Ostadrahimi, A., & Hosseinzadeh-Attar, M. J. (2020). Naringenin, a flavanone with antiviral and anti-inflammatory effects: A promising treatment strategy against COVID-19. *Phytotherapy Research: PTR*, *34*(12), 3137–3147. https://doi.org/10.1002/PTR.6781

Valdés-Tresanco, M. S., Valdés-Tresanco, M. E., Valiente, P. A., & Moreno, E. (2021). Gmx_MMPBSA: A new tool to perform end-state free energy calculations with GROMACS. *Journal of Chemical Theory and Computation*, *17*(10), 6281–6291. https://doi.org/10.1021/ACS.JCTC.1C00645/ASSET/IMAGES/LARGE/CT1C00645_0005.JPEG

Vardhan, S., & Sahoo, S. K. (2020). In silico ADMET and molecular docking study on searching potential inhibitors from limonoids and triterpenoids for COVID-19. *Computers in Biology and Medicine*, *124*, 103936. https://doi.org/10.1016/J.COMPBIOMED.2020.103936

Venkatesan, P. (2021). Repurposing drugs for treatment of COVID-19. *The Lancet Respiratory Medicine*, *9*(7), e63. https://doi.org/10.1016/S2213-2600(21)00270-8

Vieira, T. F., & Sousa, S. F. (2019). Comparing AutoDock and Vina in ligand/decoy discrimination for virtual screening. *Applied Sciences*, *9*(21), 4538. https://doi.org/10.3390/app9214538

Villas-Boas, G. R., Rescia, V. C., Paes, M. M., Lavorato, S. N., Magalhães-Filho, M. F. d., Cunha, M. S., Simões, R. d. C., Lacerda, R. B. d., Freitas-Júnior, R. S. d., Ramos, B. H. d S., Mapeli, A. M., Henriques, M. d S. T., Freitas, W. R. d., Lopes, L. A. F., Oliveira, L. G. R., Silva, J. G. d., Silva-Filho, S. E., Silveira, A. P. S. d., Leão, K. V., … Oesterreich, S. A. (2020). The New Coronavirus (SARS-CoV-2): A comprehensive review on immunity and the application of bioinformatics and molecular modeling to the discovery of potential anti-SARS-CoV-2 agents. *Molecules*, *25*(18), 4086. https://doi.org/10.3390/molecules25184086

WHO. (2021). *Classification of Omicron (B.1.1.529): SARS-CoV-2 Variant of Concern*. https://www.who.int/news/item/26-11-2021-classification-of-omicron-(b.1.1.529)-sars-cov-2-variant-of-concern

WHO. (2022). *WHO Coronavirus (COVID-19) Dashboard | WHO Coronavirus (COVID-19)* dashboard with vaccination data. https://covid19.who.int/

Wright, J. D., Sargsyan, K., Wu, X., Brooks, B. R., & Lim, C. (2013). Protein-protein docking using EMAP in CHARMM and support vector machine: Application to Ab/Ag complexes. *Journal of Chemical Theory and Computation*, *9*(9), 4186–4194. https://doi.org/10.1021/CT400508S/ASSET/IMAGES/LARGE/CT-2013-00508S_0002.JPEG

Xiong, G., Wu, Z., Yi, J., Fu, L., Yang, Z., Hsieh, C., Yin, M., Zeng, X., Wu, C., Lu, A., Chen, X., Hou, T., & Cao, D. (2021). ADMETlab 2.0: an integrated online platform for accurate and comprehensive predictions of ADMET properties. *Nucleic Acids Research*, *49*(W1), W5–W14. https://doi.org/10.1093/NAR/GKAB255

Yan, R., Zhang, Y., Li, Y., Xia, L., Guo, Y., & Zhou, Q. (2020). Structural basis for the recognition of SARS-CoV-2 by full-length human ACE2. *Science (New York, NY)*, *367*(6485), 1444–1448. https://doi.org/10.1126/SCIENCE.ABB2762/SUPPL_FILE/ABB2762S1.MP4

Zeng, W., Jin, L., Zhang, F., Zhang, C., & Liang, W. (2018). Naringenin as a potential immunomodulator in therapeutics. *Pharmacological Research*, *135*, 122–126. https://doi.org/10.1016/J.PHRS.2018.08.002